RFX6 Regulates Insulin Secretion by Modulating Ca2+ Homeostasis in Human β Cells

Vikash Chandra, Olivier Albagli-Curiel, Benoit Hastoy, Julie Piccand, Clotilde Randriamampita, Emmanuel Vaillant, Hélène Cavé, Kanetee Busiah, Philippe Froguel, Martine Vaxillaire, et al.

Article

Cell Reports

RFX6 Regulates Insulin Secretion by Modulating Ca^{2+} Homeostasis in Human β Cells

Graphical Abstract

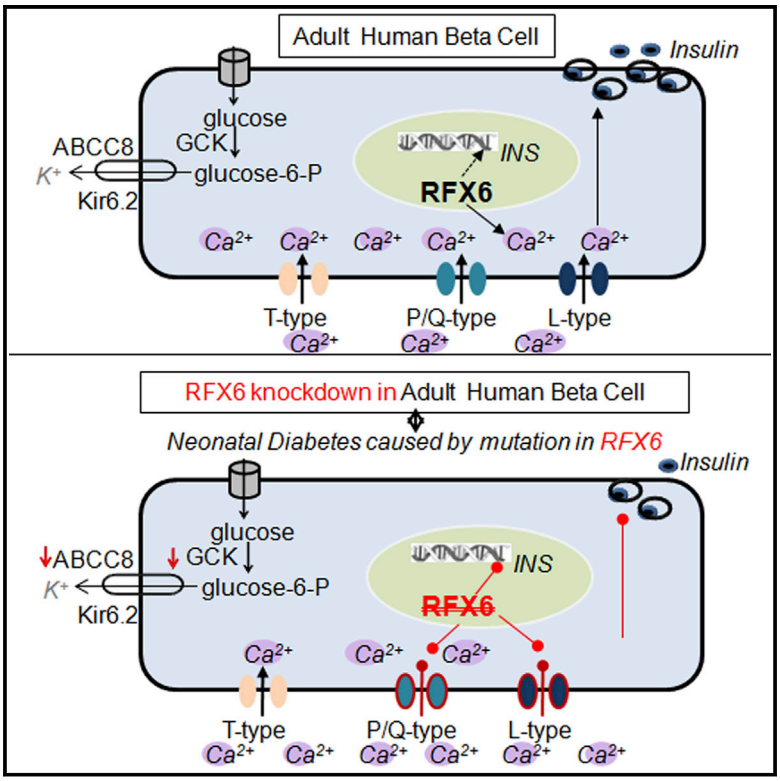

Authors

Vikash Chandra, Olivier Albagli-Curiel, ..., Michel Polak, Raphael Scharfmann

Correspondence

raphael.scharfmann@inserm.fr

In Brief

Chandra et al. show that RFX6, a transcription factor required for pancreatic endocrine cell development during prenatal life, is also expressed in mature human β cells. RFX6 controls insulin expression and secretion by modulating Ca^{2+}-channel expression.

Highlights

- RFX6 regulates insulin expression and secretion in human pancreatic β cells
- Knockdown of *RFX6* results in reduced L- and P/Q-type Ca^{2+}-channel expression
- This subsequently disturbs Ca^{2+} homeostasis and electrical activity in β cells
- This provides insight into certain forms of neonatal diabetes

Accession Numbers

GSE59049

Chandra et al., 2014, Cell Reports 9, 2206–2218
December 24, 2014 ©2014 The Authors
http://dx.doi.org/10.1016/j.celrep.2014.11.010

OPEN ACCESS
CellPress

Cell Reports
Article

RFX6 Regulates Insulin Secretion by Modulating Ca^{2+} Homeostasis in Human β Cells

Vikash Chandra,[1] Olivier Albagli-Curiel,[1] Benoit Hastoy,[2] Julie Piccand,[3] Clotilde Randriamampita,[4] Emmanuel Vaillant,[5] Hélène Cavé,[6] Kanetee Busiah,[1,7] Philippe Froguel,[5,8] Martine Vaxillaire,[5] Patrik Rorsman,[2] Michel Polak,[1,7] and Raphael Scharfmann[1,*]

[1]INSERM, U1016, Institut Cochin, Faculté de Médecine, Université Paris Descartes, Sorbonne Paris Cité, Paris 75014, France
[2]Oxford Centre for Diabetes, Endocrinology and Metabolism, University of Oxford, Churchill Hospital, Headington, Oxford OX3 7LE, UK
[3]Departement of Development and Stem Cells Program, Institute of Genetics and Molecular and Cellular Biology (IGBMC), Illkirch 67404, France
[4]CNRS, UMR8104, Institut Cochin, Paris 75014, France
[5]CNRS, UMR8199, Lille Pasteur Institute, Lille 2 University, European Genomic Institute for Diabetes (EGID), Lille 59019, France
[6]Department of Genetics, Robert-Debré Hospital, Paris 75019, France
[7]Department of Paediatric Endocrinology, Gynaecology, and Diabetology, Necker-Enfants Malades Hospital, IMAGINE Affiliate, Paris 75015, France
[8]Department of Genomics of Common Disease, School of Public Health, Imperial College London, Hammersmith Hospital, London W12 0NN, UK
*Correspondence: raphael.scharfmann@inserm.fr
http://dx.doi.org/10.1016/j.celrep.2014.11.010

SUMMARY

Development and function of pancreatic β cells involve the regulated activity of specific transcription factors. RFX6 is a transcription factor essential for mouse β cell differentiation that is mutated in monogenic forms of neonatal diabetes. However, the expression and functional roles of RFX6 in human β cells, especially in pathophysiological conditions, are poorly explored. We demonstrate the presence of RFX6 in adult human pancreatic endocrine cells. Using the recently developed human β cell line EndoC-βH2, we show that RFX6 regulates insulin gene transcription, insulin content, and secretion. Knockdown of *RFX6* causes downregulation of Ca^{2+}-channel genes resulting in the reduction in L-type Ca^{2+}-channel activity that leads to suppression of depolarization-evoked insulin exocytosis. We also describe a previously unreported homozygous missense *RFX6* mutation (p.V506G) that is associated with neonatal diabetes, which lacks the capacity to activate the insulin promoter and to increase Ca^{2+}-channel expression. Our data therefore provide insights for understanding certain forms of neonatal diabetes.

INTRODUCTION

Diabetes mellitus is a global health concern, tightly associated with the loss/dysfunction of insulin-producing pancreatic β cells. In this context, understanding the mechanisms that control β cell differentiation and function represents a major challenge. Pancreatic β cell differentiation involves the regulated sequential expression of specific transcription factors (reviewed in Arda et al., 2013; Pan and Wright, 2011). Interestingly, a number of transcription factors involved in pancreogenesis continue to be expressed in terminally differentiated β cells, where they control and maintain β cell function. Examples include *PDX1* (Ahlgren et al., 1998; Gao et al., 2014), *NKX2.2* (Doyle and Sussel, 2007; Papizan et al., 2011), and *NKX6.1* (Taylor et al., 2013). Mutations in some of such pancreatic transcription factors have been associated with monogenic forms of diabetes in humans, demonstrating their key role in islet function (reviewed in Folias and Hebrok, 2014; Polak and Shield, 2004; Vaxillaire et al., 2012).

RFX6, a winged helix transcription factor, is a member of regulatory factor X (RFX) family, an evolutionarily conserved DNA binding protein family, that associate with a conserved *cis*-regulatory element called the X box motif (Aftab et al., 2008). Recent studies demonstrate that RFX6 is necessary for islet cell differentiation during embryonic pancreatic development in mice (Smith et al., 2010; Soyer et al., 2010). Such studies also indicate that the expression of RFX6 is maintained in adult mouse β cells. However, *RFX6* knockout mice die within 2 days after birth, and hence knowledge on the functional role of RFX6 in mature mouse β cells is limited (Smith et al., 2010). Biallelic mutations in *RFX6* were previously reported to be responsible for a rare monogenic form of neonatal diabetes in human associated with other digestive system defects (known as the Mitchell-Riley syndrome [OMIM #601346]) (Concepcion et al., 2014; Smith et al., 2010; Spiegel et al., 2011), but the underlying pathophysiological mechanisms remain largely unknown.

Data obtained from mouse studies have previously been successfully extrapolated to explain human β cell pathophysiology (Caicedo, 2013; Folias and Hebrok, 2014). However, whereas mouse and human β cells share many similarities, they also differ in many respects such as insulin expression, glucose transport,

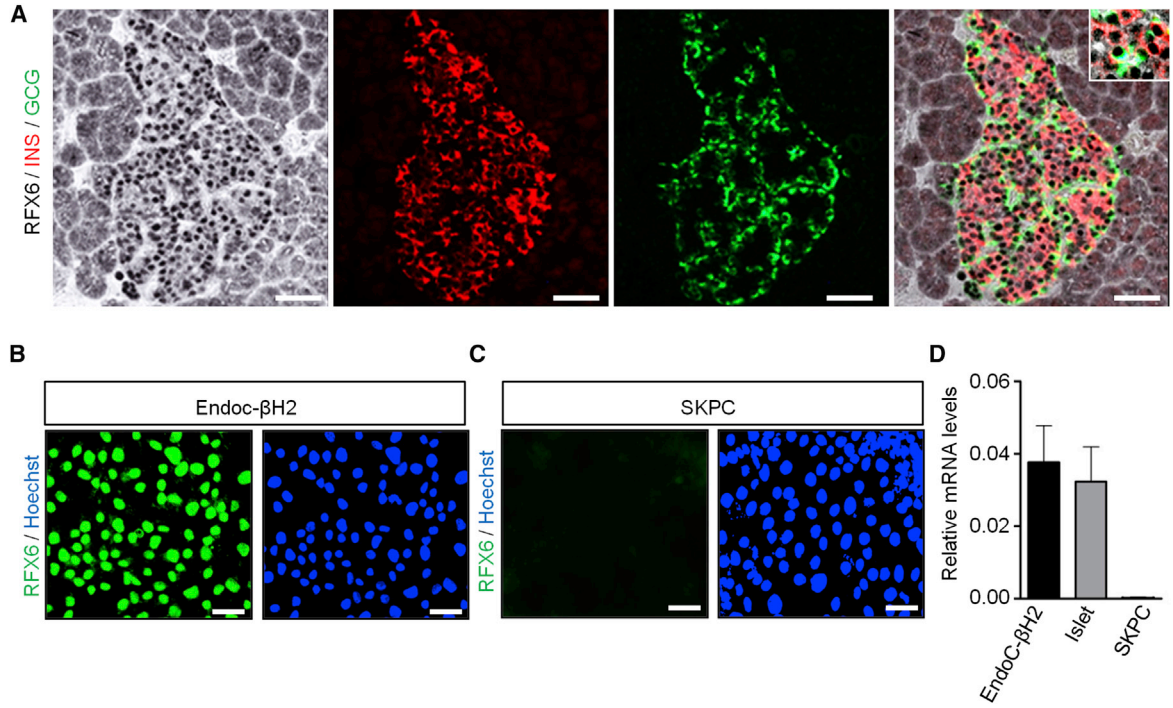

Figure 1. Expression of RFX6 in Adult Human Pancreas and in EndoC-βH2 Cells

(A) Immunohistochemical analysis of formalin-fixed human adult pancreatic sections stained for RFX6 (black), insulin (INS in red) and glucagon (GCG in green). RFX6 is expressed in the islets in the nuclei of β (INS) and alpha (GCG) cells (see inset). Scale bars, 25 μm.

(B and C) Immunofluorescence analysis of RFX6 expression in EndoC-βH2 and SKPC cells. Nuclear expression of RFX6 (in green) is observed in EndoC-βH2 but not in the duct cell line SKPC. Nuclei are stained with Hoechst 33342 stain (blue). Scale bars, 50 μm.

(D) Real-time qPCR comparison of the relative levels of *RFX6* transcripts between EndoC-βH2, adult human islets, and SKPC (used as negative control).

ion channels for Ca^{2+}-mediated insulin exocytosis, and electrical properties (Caicedo, 2013; Rorsman and Braun, 2013; Scharfmann et al., 2013) or the expression of specific transcription factors such as MAFB, which is absent from rodent mature β cells, but expressed in human β cells (Dai et al., 2012; Dorrell et al., 2011).

In the present study, we explored the role of RFX6 in human β cells. We used the human β cell line EndoC-βH2 (Scharfmann et al., 2014). We show that knockdown of *RFX6* results in reduced insulin gene transcription and an impaired glucose-stimulated insulin secretion. We applied transcriptome analysis to identify RFX6 target genes. We also provide evidence that a previously unreported homozygous missense mutation of *RFX6* is very likely the cause of human neonatal diabetes by affecting Ca^{2+}-channel expression. Collectively, the data we report here suggest that RFX6 plays a key role in human β cells.

RESULTS

RFX6 Is Highly Expressed in Adult Human Pancreatic Islets and in the Human β Cell Line EndoC-βH2

The expression of RFX6 in the adult mouse pancreas is well established (Smith et al., 2010; Soyer et al., 2010); however, less is known about its expression in the adult human pancreas. Immunostaining for RFX6 on human adult pancreatic sections showed nuclear localization of RFX6 in both human beta (insulin$^+$) and alpha (glucagon$^+$) cells (Figure 1A). Immunostaining of EndoC-βH2 cells revealed nuclear localization of RFX6, which was absent in the human duct cell line SKPC (Figures 1B and 1C). Real-time quantitative PCR (qPCR) analysis showed expression of *RFX6* transcripts in adult human islets and EndoC-βH2 but not in SKPC duct cell line, which further confirms the selective expression of RFX6 in endocrine cells in the human pancreas (Figure 1D).

RFX6 Loss of Function Affects Insulin Expression and Secretion

To define the role of RFX6 in adult human β cells, we used small interfering RNA (siRNA)-based loss-of-function studies in the human β cell line EndoC-βH2. We devised a modified reverse transfection protocol to achieve >90% transfection efficiency as confirmed by flow cytometry using a fluorescent oligonucleotide duplex (Figure S1A). Using this approach, we efficiently (>70%) decreased RFX6 expression in EndoC-βH2 both at the transcript (Figure 2A) and protein (Figures 2B and 2C) levels. Decreased *RFX6* expression was paralleled by a 59% ± 10% decrease in insulin mRNA levels (Figure 2D) and a 88% ± 8% reduction of a 5′ intron-2-containing preinsulin mRNA (Figure 2E), the latter being a reliable reflection of human insulin transcription rate (Evans-Molina et al., 2007). siRFX6-transfected cells also showed a 54% ± 3.75% reduction in the activity of the human insulin promoter as compared to control cells, supporting a role for RFX6 in

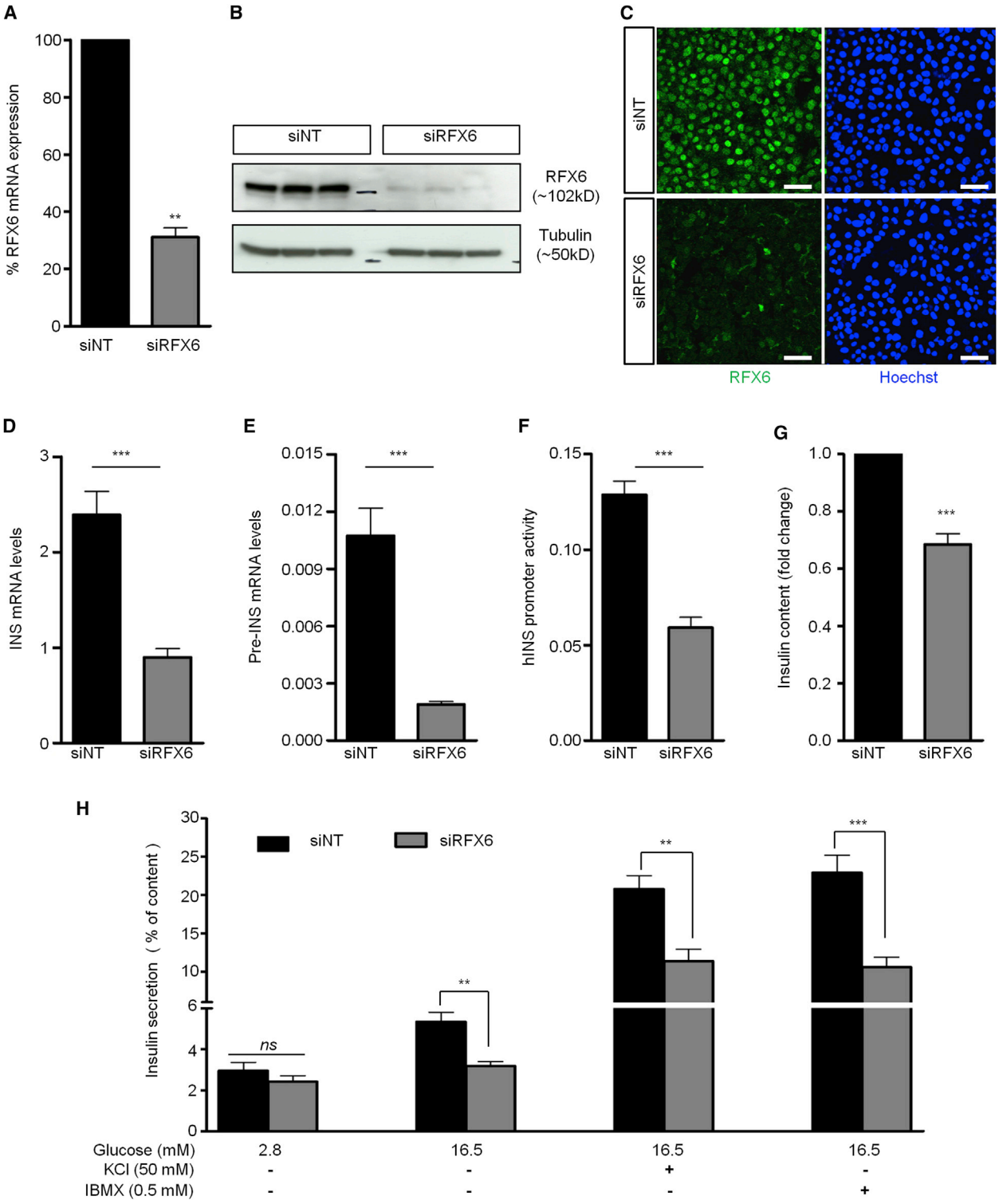

Figure 2. *RFX6* Knockdown in EndoC-βH2 Cells Leads to Impaired Insulin Expression and Secretion

EndoC-βH2 cells were transfected with control nontarget siRNA (siNT) or siRNA targeting *RFX6* (siRFX6) and analyzed 72 hr posttransfection.

(A) *RFX6* mRNA expression was determined by real-time qPCR. Results are presented relative to *RFX6* expression in siNT-transfected cells.

(B) Immunoblot analysis of RFX6 expression in EndoC-βH2 cells transfected with siNT or with siRFX6. Tubulin was used as loading control. Data from three independent transfections are presented.

(legend continued on next page)

the control of insulin gene transcription (Figure 2F). At the same time, in agreement with a reduction in insulin transcripts, the total insulin content was reduced by 31% ± 10% in siRFX6-transfected EndoC-βH2 cells (Figure 2G).

Next, we studied the impact of *RFX6* knockdown on insulin secretion. *RFX6* knockdown did not affect the basal insulin secretion measured at 2.8 mM glucose. However, insulin secretion evoked by 16.5 mM glucose was strongly inhibited in siRFX6-treated cells as compared to siNT-treated control cells (Figure 2H). Glucose-induced insulin secretion expressed as percentage of insulin content (to compensate for the moderate reduction of insulin content) was nearly abolished following knockdown of *RFX6*. Insulin secretion evoked by 50 mM K^+ (to depolarize the EndoC-βH2 cells and open voltage-gated Ca^{2+} channels) or 0.5 mM of the phosphodiesterase inhibitor 3-isobutyl-1-methylxanthine (IBMX) was likewise strongly inhibited (Figure 2H). Thus, both insulin gene expression and secretion are decreased following *RFX6* knockdown in human β cells.

RFX6 Regulates Calcium Channels Encoding Genes in EndoC-βH2 Cells

Transcriptome microarray analysis was performed between siNT control- and siRFX6-treated EndoC-βH2 cells. It confirmed a significant downregulation of *RFX6* transcript in siRFX6 samples (fold change [FC] −2.38; $p = 3.75 \times 10^{-6}$). *RFX6* knockdown had no major impact on the expression of several genes encoding β cell transcription factors such as *PDX1*, *MAFB*, *NEUROD*, *PAX6*, and *NKX2-2* (Figures S1B and S1C). However, there was significant downregulation of transcripts mostly associated with distal events of glucose sensing in siRFX6-transfected EndoC-βH2 cells. Thus, the expression of *GCK* (FC, −1.55; $p = 9.8 \times 10^{-5}$) and the sulphonylurea receptor 1 (*ABCC8*; FC, −1.50; p = 0.01), a subunit of the K_{ATP} channel, was decreased. The expression of many of the voltage dependent Ca^{2+} channels present in human β cells (Braun et al., 2008) was markedly reduced: Ca^{2+}-channel genes affected include the P/Q-type Ca^{2+} channels (*CACNA1A*; FC, −2.39; p = 0.006), L-type Ca^{2+} channels (*CACNA1C*; FC, −1.48; $p = 6.4 \times 10^{-5}$ and *CACNA1D*; FC, −1.25; $p = 5.0 \times 10^{-4}$), and the Ca^{2+}-channel beta-2 subunit (*CACNB2*; FC, −2.02; $p = 1.8 \times 10^{-6}$). These results were validated by real-time qPCR: *GCK* (42% ± 3%), *ABCC8* (41% ± 16%), *CACNA1A* (64% ± 11%), *CACNB2* (70% ± 15%), *CACNA1C* (55% ± 11%), and *CACNA1D* (46% ± 3%; Figure 3). The reduced *ABCC8* expression was paralleled by a corresponding decrease in the expression of Kir6.2 (*KCNJ11*), the pore-forming subunit of the K_{ATP} channel, but this decrease did not attain statistical significance. No significant difference was observed for T-type Ca^{2+} channel (*CACNA1H*) by either microarray or by real-time qPCR analysis (Figure 3) indicating that the RFX6 transcription factor might be specifically involved in the regulation of P/Q type and L type calcium channels in human β cells. Collectively, these data indicate significant perturbation of the expression of Ca^{2+}-channel subunits following decreased *RFX6* expression. Importantly, similar data were observed upon siRNA-mediated *RFX6* depletion in human islets (Figure S2).

To confirm these results, we fused the *trans*-repressing KRAB domain (Margolin et al., 1994) to RFX6 followed by an IRES-EGFP cassette (Figure S3A). We then asked whether this construct could indeed decrease the expression of the RFX6 regulated genes highlighted by the analyses in Figure 3. EndoC-βH2 cells were transfected with either a vector encoding KRAB-RFX6-IRES-EGFP or with the control KRAB-IRES-EGFP vector. GFP-positive cells were fluorescence-activated cell sorting (FACS) isolated. Real-time qPCR analyses indicated significant decrease in the expression of Pre-*INS*, *INS*, *GCK*, *ABCC8*, and *CACNA1A* in KRAB-RFX6-expressing cells (Figures S3B–S3G). The expression of *CACNA1C* transcripts also decreased but did not attain statistical significance (data not shown). These findings further strengthen the hypothesis of a regulation of these genes by RFX6 in human β cells.

RFX6 Knockdown Reduces L-type Ca^{2+}-Channel Activity and Insulin Exocytosis in EndoC-βH2 Cells

Ca^{2+}influx by VDCC is a major regulator of insulin secretion cascade in β cells (Rorsman and Braun, 2013). Whereas the L-type Ca^{2+} channel blocker nifedipine decreased glucose-stimulated insulin secretion in siNT-control cells, it was without effect in siRFX6-treated cells (Figure 4A). This would be consistent with the L-type Ca^{2+} channels not being expressed in EndoC-βH2 cells lacking RFX6. To directly study the effect of reduced *RFX6* expression on Ca^{2+} handling, we next monitored glucose- (Figure 4B) and high K^+-evoked changes in $[Ca^{2+}]_i$ (Figure 4C). Such effects of glucose on calcium flux were also confirmed by real-time visualization of intracellular calcium dynamics in control siNT- and siRFX6-transfected cells using fluorescent Ca^{2+} sensitive dye (Fura-4NW; Movies S1, S2, S3, and S4). These experiments showed that the responses to both stimulation paradigms were attenuated in siRFX6-transfected cells compared to siNT-control cells.

The impact of knockdown of *RFX6* on Ca^{2+}-channel expression was examined further by electrophysiological studies. Figure 5A shows Ca^{2+} currents recorded from EndoC-βH2 transfected with control siRNA (siNT) and siRFX6 during depolarizations from −70 mV to zero mV. The current-voltage

(C) Immunofluorescence comparison of RFX6 (green) expression in siNT- and siRFX6-transfected cells. Nuclei are stained with Hoechst 33342 stain (blue). Scale bars, 50 μm.

(D and E) Real-time qPCR analysis of *INS* and Pre-INS mRNA expression, in siNT- and siRFX6-transfected cells.

(F) Insulin promoter activity was determined by firefly luciferase (pGL4.12hu*INS*-378to+42) and normalized to *Renilla* luciferase (pGL4.72-TK[hRlucCP]) in EndoC-βH2 cells transfected with either siNT or with siRFX6.

(G) Cellular insulin content was quantified by ELISA in siNT- and siRFX6-transfected cells and normalized to total protein content. Results are represented as fold change over siNT.

(H) Insulin secretion (percentage of secretion of the total insulin content) in response to 1 hr incubations with 2.8 mM glucose, 16.5 mM glucose, 16.5 mM glucose + 50 mM KCl, and 16.5 mM glucose + 0.5 mM IBMX in siNT- and siRFX6-transfected EndoC-βH2 cells, 72 hr posttransfection.

Data represent mean values of at least three independent experiments. Data are mean ± SEM. **p < 0.01; ***p < 0.001; and *ns*, not significant.

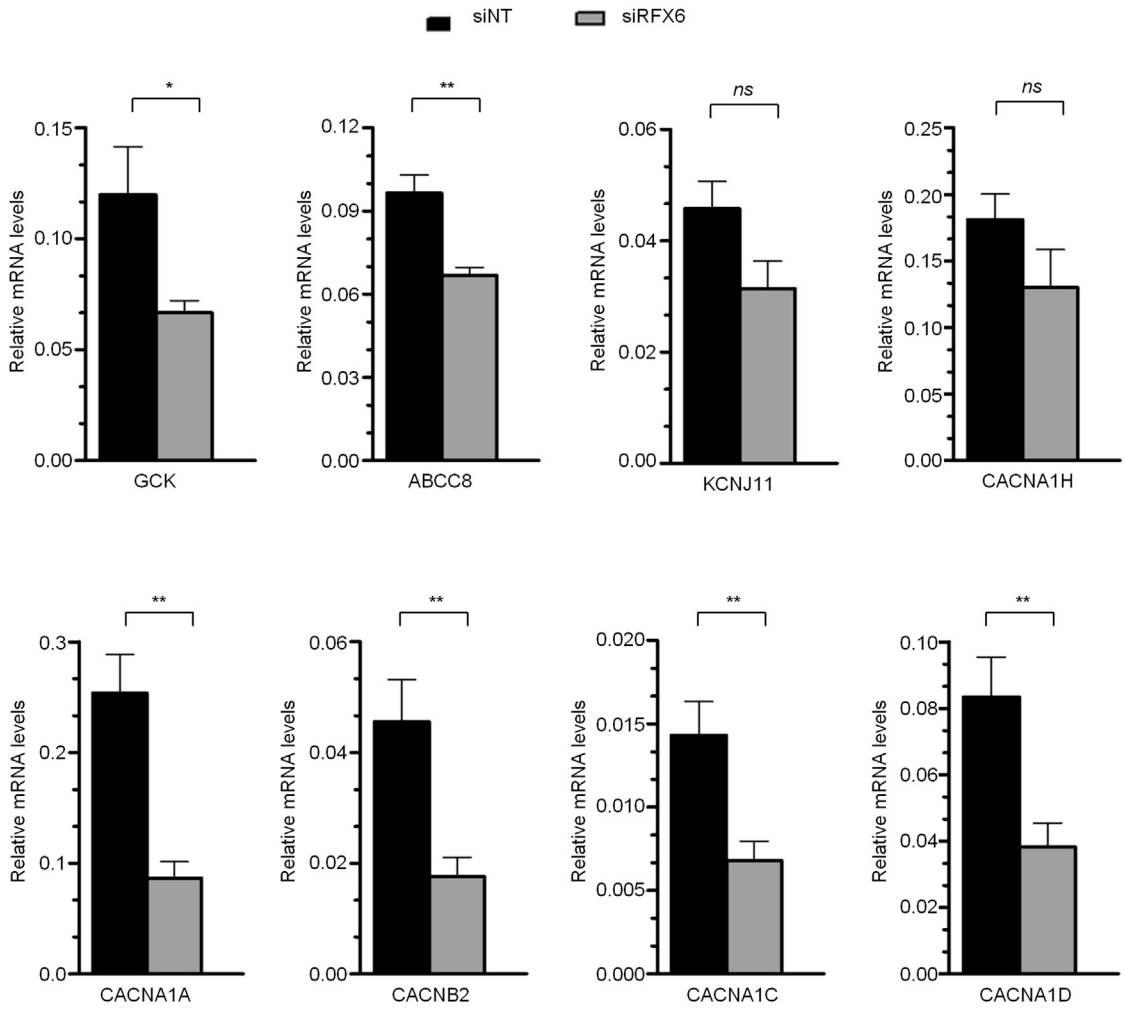

Figure 3. Transcriptome Analysis of *RFX6* Knockdown EndoC-βH2 Cells

Validation by real-time qPCR of selected genes whose expression was found decreased in transcriptome microarray analysis in siRFX6-transfected EndoC-βH2 cells compared to control cells. Data represent mean values of four independent siNT or siRFX6 transfections. Data are mean ± SEM. *$p < 0.05$; **$p < 0.01$; and *ns*, not significant.

relationship shown to the right summarizes the effects of reduced *RFX6* expression on Ca^{2+} currents evoked by voltage steps between −80 and +40 mV. Inward currents become detectable during depolarization to −40 mV and above and are maximal at membrane potentials between zero and +10 mV. The peak amplitude in control EndoCβ-H2 is ~8 pA/pF, marginally lower than the ~10 pF seen in primary human β cells (Braun et al., 2008). After knockdown of *RFX6*, the peak Ca^{2+}-current was reduced by 40% and averaged 5 pA/pF. The whole-cell capacitance averaged 9.1 ± 1.0 pF (n = 16) and 12.5 ± 1.2 pF (n = 18; $p < 0.05$).

For the subsequent analysis, Ca^{2+} currents were evoked by voltage ramps between −80 and +40 mV (Figure 5B). The current amplitudes, shape of the current-voltage relationship, as well as the effects of knockdown of *RFX6* derived from these measurements were identical to those obtained during step depolarizations. We measured the charge normalized by the size of the cell between −20 and +20 mV. On average, this was reduced by ~50% in cells treated with siRFX6 (Figure 5B).

We used the blockers ω-agatoxin and isradipine to pharmacologically isolate the P/Q- and L-type Ca^{2+}-current components, respectively. Figures 5C and 5D show the relative contribution of the L- (Figure 5C) and P/Q-type Ca^{2+} currents (Figure 5D) evoked by the voltage ramp protocols. Currents are expressed as percentage of the control current. The isradipine-sensitive L-type Ca^{2+}-current component accounts for ~45% of the total current in EndoCβ-H2 cells transfected with control siRNA. This is reduced to ~25% after knockdown of *RFX6*. The current-voltage relationship of the isradipine-sensitive current is fairly broad with and clearly biphasic in cells with reduced *RFX6* expression, possibly indicative of the block expression of two L-type Ca^{2+}-channel genes (*CACNA1C* and *CACNA1D*) that activate at slightly different voltages. The area under the curve between −30 and +30 mV was reduced by 50% in

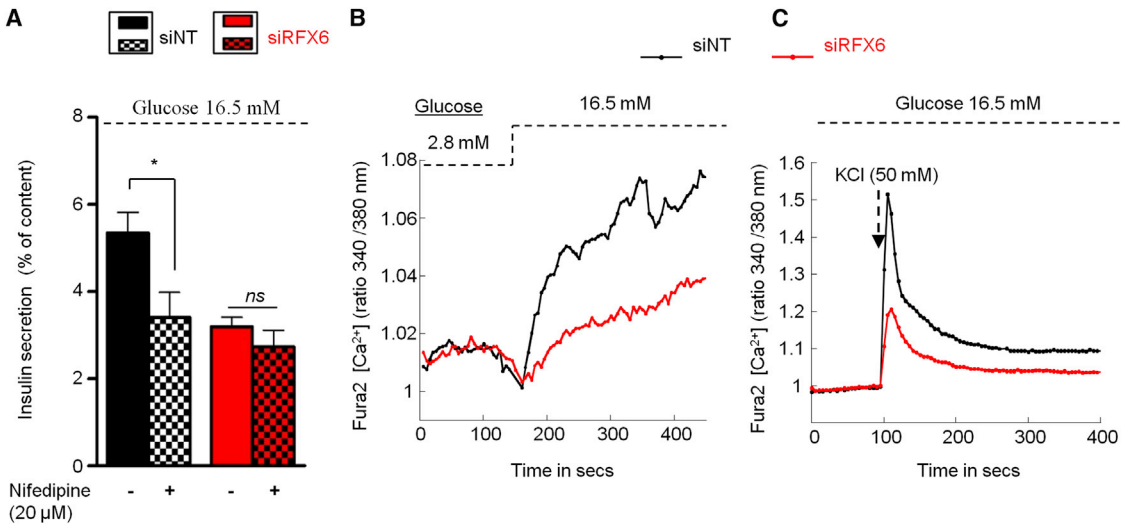

Figure 4. *RFX6* Knockdown Impairs Ca^{2+} Responses in EndoC-βH2 Cells

(A) EndoC-βH2 cells were transfected with siNT or siRFX6. After 72 hr, cells were incubated for 1 hr in 16.5 mM glucose with or without 20 μM of the L-type Ca^{2+}-channel blocker nifedipine, and insulin secretion was measured. Data are mean ± SEM. *$p < 0.05$; *ns*, not significant.

(B and C) Ratiometric fura-2 measurements of $[Ca^{2+}]_i$. Data are shown as the 340/380 nm fluorescence ratio in EndoC-βH2 treated with siNT (black line) or siRFX6 (red line). Measurements were conducted 72 hr after transfection. In (B), cells were incubated with 2.8 mM glucose and then stimulated with 16.5 mM glucose as indicated. In (C), cells were treated with 50 mM KCl in the presence of 16.5 mM glucose. Calcium traces represent the mean responses of 50–70 individual cells. Data represent mean values of at least three independent experiments.

siRFX6-treated cells compared to control (siNT) cells. When the same analysis was repeated for the ω-agatoxin-sensitive component (representing P/Q-type Ca^{2+} channels), downregulation of *RFX6* had no detectable inhibitory effect (Figure 5D).

Insulin exocytosis is a Ca^{2+}-dependent process that depends on Ca^{2+} influx via L-type Ca^{2+}-channel activity. We examined the impact reduced L-type Ca^{2+}-channel activity due to downregulation of *RFX6* by performing high-resolution capacitance measurements. Exocytosis (measured in fF) evoked by a train of ten 500 ms depolarizations was reduced by 75% after downregulation of *RFX6* (Figure 5E), from 36 ± 9 (n = 6) to 9 ± 2 fF/pF (n = 5; $p < 0.03$). We also analyzed the exocytotic response for the individual pulses during the train (Figure 5F). In agreement with findings in primary human β cells (Braun et al., 2009), the magnitude of the individual exocytotic responses in control cells (siNT) declines by ~80% during the train. The suppressor effect of siRFX6 on depolarization-evoked exocytosis is particularly pronounced during the initial part of the train of stimulations, and only the reduction of the response to the first pulse actually approached statistical significance ($p = 0.05$). This effect is very similar to that previously observed in mouse β cells following blockade or genetic ablation of L-type Ca^{2+} channels (Schulla et al., 2003).

We ascertained that the reduction of exocytosis is not simply due to reduced granule density. We determined the number of docked insulin granules by TIRF microscopy. The average granule density was 0.23 ± 0.03 granule/μm^2 for the control (n = 10) and 0.16 ± 0.03 granule/μm^2 for the cells transfected with siRFX6 (n = 9). This decrease of ~30% (not statistically significant) is comparable to the reduction of insulin content and insufficient to account for the much greater (>80% during first pulse of train) suppression of depolarization-evoked exocytosis.

Collectively, the observations in Figures 4 and 5 suggest that the reduction of glucose-induced insulin secretion resulting from downregulation of *RFX6* principally results from reduced L-type Ca^{2+}-channel activity.

Characterization of a Missense *RFX6* Mutation Associated with Neonatal Diabetes

We studied a patient with neonatal diabetes and intestinal developmental abnormalities. The patient is now 6 years old and is treated with insulin injections (average insulin ~0.6 units/kg/day). A detailed description of the patient phenotype is presented in Table S1. The SNP-microarray homozygosity mapping analysis showed a total of 14 genomic runs of homozygosity (ROH) segments larger than 2.5 Mb in the proband's genome, after filtering the overlapping ROHs from the father and the mother. One of these ROH regions mapped to chromosome 6q21–q22 (from rs9374311 to rs1494137, totaling 13,239 Mb in size) and encompassed the whole genomic sequence of *RFX6*. Therefore, and on the basis of the phenotype features of the patient, we sequenced the exons, splicing junctions, and proximal promoter of *RFX6* gene in the proband. A homozygous missense mutation in exon 14 of *RFX6* giving rise to Val to Gly change at amino acid 506(c.1517T > G, p.V506G; transcript number: NM_173560.3) was identified in the patient (Figure S4A). Both parents were found to be heterozygous carriers of the same mutation. The *RFX6*p.V506G mutation was not previously reported by either the 1,000 Genomes Project or the NHLBI Exome Sequencing Project.

By aligning the amino acid sequences of RFX6 homologs in different species, we found that the mutated valine at position p.506 is highly conserved among homologs, being present in

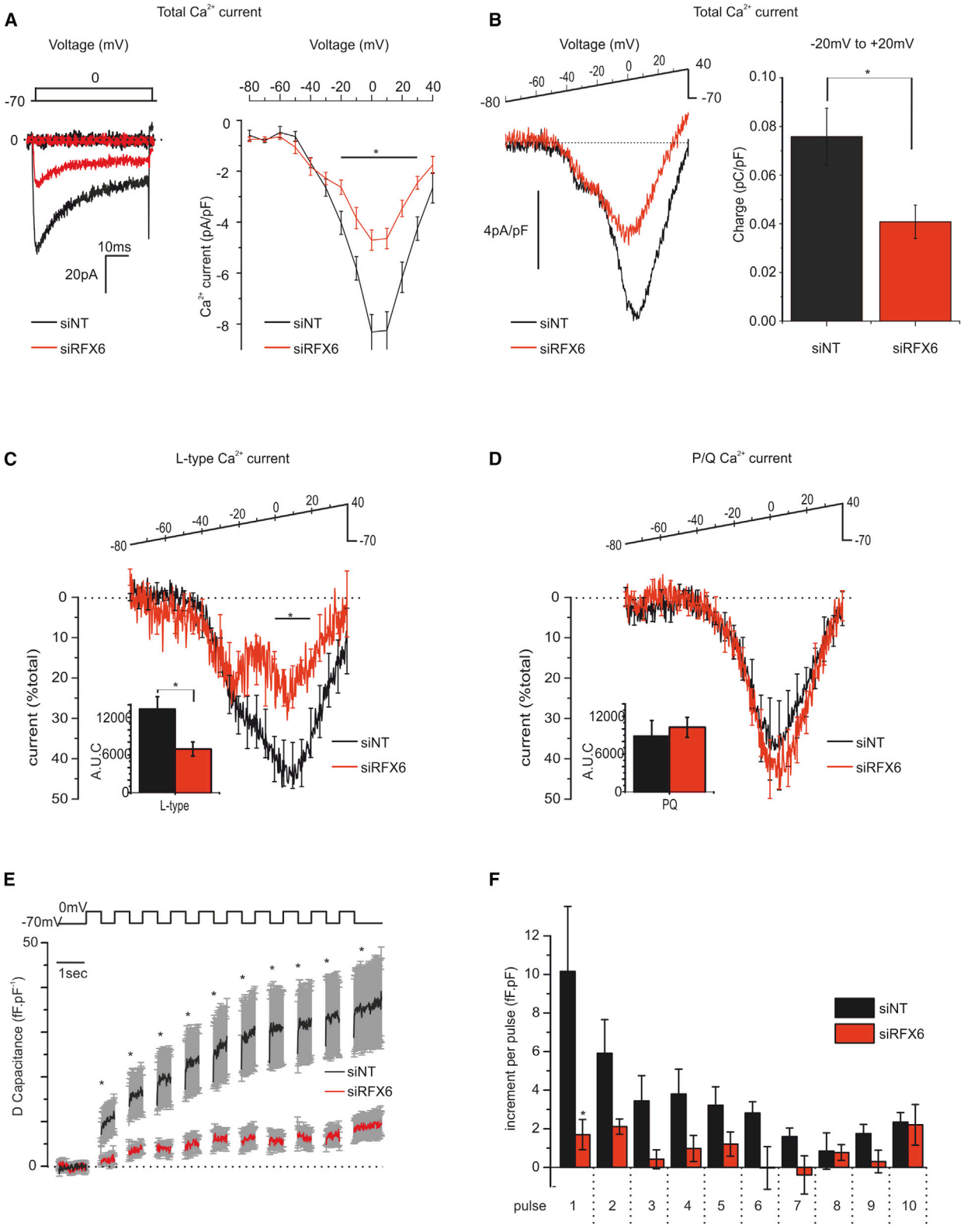

Figure 5. Effect of *RFX6* Downregulation on Ca^{2+} Currents

(A) Total Ca^{2+} currents elicited by depolarization from −80 mV to +40 mV for 50 ms. Raw traces observed at −70 and 0 mV are on the left and current-voltage relationship on the right (siNT n = 10, siRFX6 n = 13; $p < 0.05$ for voltages indicated by horizontal line).

(legend continued on next page)

RFX genes in highly distant metazoans from hydra to human (Figure S4B). This residue maps within a region termed dimerization domain (D), which is also highly conserved in a subset of RFX paralogs (RFX1-RFX4; Figure S4C) (Emery et al., 1996). This D domain plays an important role in homo- and heterodimerization between RFX proteins (Reith et al., 1990).

We tested in EndoC-βH2 the effect of this mutation on insulin and calcium-channel expression. Our above-described results indicate that knockdown of *RFX6* in EndoC-βH2 cells resulted in a decrease in insulin transcription (Figure 2). The human insulin promoter contains X box motifs as potential RFX binding sites (Figures 6A, 6B, and S5). We cotransfected the human insulin promoter fragment (−378 to +42) driven luciferase reporter gene with either wild-type RFX6 (wtRFX6) or RFX-p.V506G mutant (Mut506RFX6) into EndoC-βH2 cells (Figure 6C). Although wtRFX6 significantly increased luciferase activity (10 ± 2-fold), Mut506RFX6 was unable to do so (Figure 6D). We investigated the ability of either wtRFX6 or Mut506RFX6 to rescue the activity of the insulin promoter in RFX6-depleted cells. Accordingly, we cotransfected either wtRFX6 or Mut506RFX6 with the insulin promoter in siRFX6-treated cells. Whereas the activity of the insulin promoter is recovered in cells transfected with wtRFX6, this was not in cells expressing Mut506RFX6 (Figure 6E). Four potential X box motifs are detected within 3 kb of the insulin promoter (Figure S5). We cloned them in two times into pGL4.25 (*luc2CP*/minP) luciferase vector and assessed activation by VP16-conjugated RFX6 or VP16-conjugated Mut506RFX6. VP16-conjugated constructs were validated first on human insulin promoter fragment (−378 to +42; Figure S6A). Interestingly, among the four mentioned X box motifs, −288 X box motif was the only one activated by VP16-conjugated RFX6. Importantly, VP16-conjugated Mut506RFX6 was unable to activate −288 X box motif (Figure S6B).

We finally performed gain-of-function experiments in EndoC-βH2 cells to compare the effect of wild-type and Mut506RFX6. EndoC-βH2 cells were transfected with IRES-EGFP bicistronic vectors encoding either wtRFX6 or Mut506RFX6 (Figure 7A), and, 48 hr later, FACS-isolated GFP-positive cells were analyzed by real-time qPCR for calcium-channel gene expression. Wild-type and mutant *RFX6* mRNA levels were expressed at a similar level in transfected cells (Figure 7B). Under these conditions, neither normal RFX6 nor Mut506RFX6 were able to increase insulin mRNA levels suggesting that endogenous RFX6, which is expressed at high levels in EndoC-βH2 cells, is saturating in the assay (data not shown). However, overexpression of wtRFX6 significantly increased *CACNA1A*, *CACNB2*, and *CACNA1D*, which is not observed upon Mut506RFX6 expression (Figures 7C–7F). We conclude that Mut506RFX6 has lost the ability to positively regulate P/Q- and L-type Ca^{2+}-channel genes in pancreatic β cells.

DISCUSSION

Recent studies have demonstrated the pivotal role of the transcription factor RFX6 in endocrine cell differentiation during pancreas development (Smith et al., 2010; Soyer et al., 2010). However, less is known on its function in mature β cells. Here, we have addressed the functional consequences of ablating RFX6 in a glucose-responsive insulin-secreting human β cell line (EndoC-βH2) that expresses all the genes expected to be found in human primary β cells (Scharfmann et al., 2014). We also validated the use of EndoC-βH2 cell line to understand why a human RFX6 mutant gives rise to neonatal diabetes in human. The use of a human β cell model is essential because accumulating evidence indicates major and significant differences between rodent and human β cells (Caicedo, 2013; Rorsman and Braun, 2013; Scharfmann et al., 2013).

Here, we demonstrate that the transcription factor RFX6 is expressed in human pancreatic β cells in agreement with previous finding in rodents (Smith et al., 2010; Soyer et al., 2010) and that it regulates insulin gene expression and insulin secretion. The latter effect is mediated by controlling the expression of genes encoding the voltage-gated Ca^{2+} channels that are linked to β cell electrical activity and insulin exocytosis. Moreover, we found that a biallelic mutant form of RFX6, which is associated with neonatal diabetes in human, has lost the ability to activate the insulin promoter and the expression of calcium channels.

RFX6 depletion from EndoC-βH2 cells using siRNA decreased insulin mRNA levels and insulin content. This decrease is transcriptional as level of expression of intron-2-containing insulin pre-mRNA, a reliable readout for human insulin gene transcriptional rate (Evans-Molina et al., 2007) as well as the activity of an isolated insulin promoter decreased following siRNA-mediated RFX6 depletion. This regulation could be mediated by the binding of RFX6 to an X box motif on the INS promoter. We have identified four potential X-box sites (Figures 6A and S5). Two of the X box consensus sequences with high matrix similarity (at −288 and −308) are located within a region of ∼400 bp upstream to the transcriptional start site, a major regulatory region within the insulin promoter (Hay and Docherty, 2006). When we tested individually these four X box motifs, −288 motif was the only one that responded to VP16-conjugated RFX6, whereas it was insensitive to VP16-conjugated Mut506RFX6. Altogether, these data indicate that RFX6 regulates insulin gene transcription and content within human β cells.

(B) Ca^{2+} currents evoked by voltage ramps between −80 and +40 mV. Representative traces normalized by cell capacitane (approximate cell size) are shown. The histogram summarizes the data of several experiments of the type illustrated to the left. Data represent the charge of the cell between −20 and +20 mV for cells transfected with siNT (n = 6) or siRFX6 (n = 7; $p < 0.05$).

(C) Net L-type Ca^{2+}-current isolated by subtracting currents recorded in the presence of isradipine (10 μM) from that observed prior to the addition of the antagonist. Net currents were normalized to the control current recorded in the absence of isradipine (= 100%), and traces shown represent averages from five (siNT) and four (siRFX6) cells. Data are mean ± SEM. For clarity, SEM values are shown for every 5 mV. Inset shows AUC between −30 and +30 mV. *$p < 0.05$.

(D) Net P/Q-type Ca^{2+}-current isolated and analyzed as described in (C) but using 200 nM ω-agatoxin IVA. Data were obtained in five cells transfected with siNT and seven cells transfected with siRFX6.

(E) Exocytosis (measured as cumulative increase in membrane capacitance, ΔC) elicited by a train of ten 500 ms depolarizations from −70 mV to 0 mV applied at 1 Hz. Data are mean ± SEM of six cells transfected with siNT and five cells transfected with siRFX6 ($p < 0.05$ as indicated).

(F) Capacitance increase for each depolarization displayed against pulse number. Same data as in (E). $p = 0.05$.

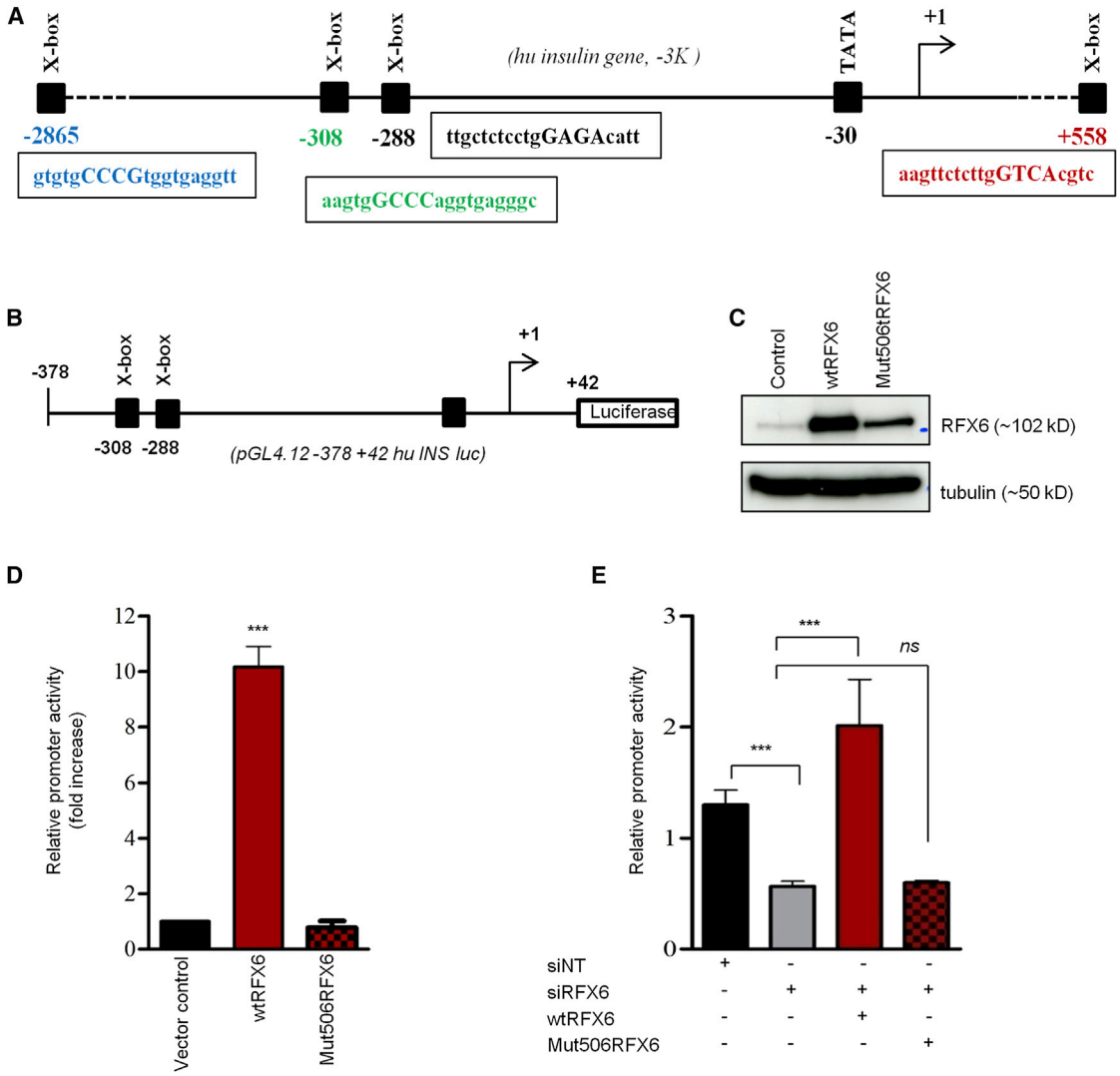

Figure 6. WT, but Not Mut506RFX6, Transactivates the Insulin Promoter in EndoC-βH2 Cells

(A) Schematic representation of the *INS* gene promoter showing potential RFX binding sites (X box motifs) identified with MatInspector (Genomatix software). Number refers to nucleotide position upstream of transcription start site.

(B) The human insulin promoter region −378 to +42 was cloned into pGL4.12 (*luc2CP*) basic vector.

(C) Western blot analysis of RFX6 in total cellular protein extracts from control, pcDNA3.1+RFX6, and pCDNA3.1+Mut506RFX6-transfected EndoC-βH2.

(D) Insulin promoter activity in EndoC-βH2 cells determined by firefly luciferase (pGL4.12hu*INS*-378to+42), which was cotransfected with either wtRFX6 or Mut506RFX6 and with *Renilla* luciferase (pGL4.72-TK[hRlucCP]) to correct for variation in transfection efficiency. Results are presented as fold increase over empty control vector.

(E) Wild-type RFX6, but not Mut506RFX6, rescues insulin promoter activity in siRFX6-transfected EndoC-βH2 cells. Cells were transfected with siNT or siRFX6. After 72 hr, siRFX6-transfected cells were transfected with either RFX6 or Mut506RFX6 + firefly luciferase (pGL4.12hu*INS*-378to+42) and *Renilla* luciferase (pGL4.72-TK[hRlucCP]). Luciferase assay was performed 24 hr later.

Data represent mean values of at least three independent experiments. Data are mean ± SEM. ***$p < 0.001$; *ns*, not significant.

Glucose-stimulated insulin secretion requires its intracellular uptake and metabolic degradation, ATP production, closure of ATP-dependent K^+ (K_{ATP}) channels, cell depolarization, and opening of voltage-gated Ca^{2+} channels that gives rise to calcium entry (Rorsman, 1997). Interestingly, siRNA-mediated depletion of RFX6 led to complete inhibition of glucose-stimulated insulin secretion. Fluorimetric measurements of glucose-induced $[Ca^{2+}]i$ changes suggest that this is due to reduced Ca^{2+} entry. Importantly, glucose still elevated $[Ca^{2+}]_i$ in RFX6-depleted EndoC-βH2 cells (Figure 4B). This indicates that the "triggering" (K_{ATP}-channel-dependent) effect of glucose remained intact after RFX6 silencing. This would be consistent with a lowered expression of the K_{ATP}-channel genes encoding the two SUR1 (*ABCC8*) and Kir6.2 (*KCNJ11*). Reduced K_{ATP}-channel expression/activity would increase electrical excitability, an effect that may offset any reduced metabolism

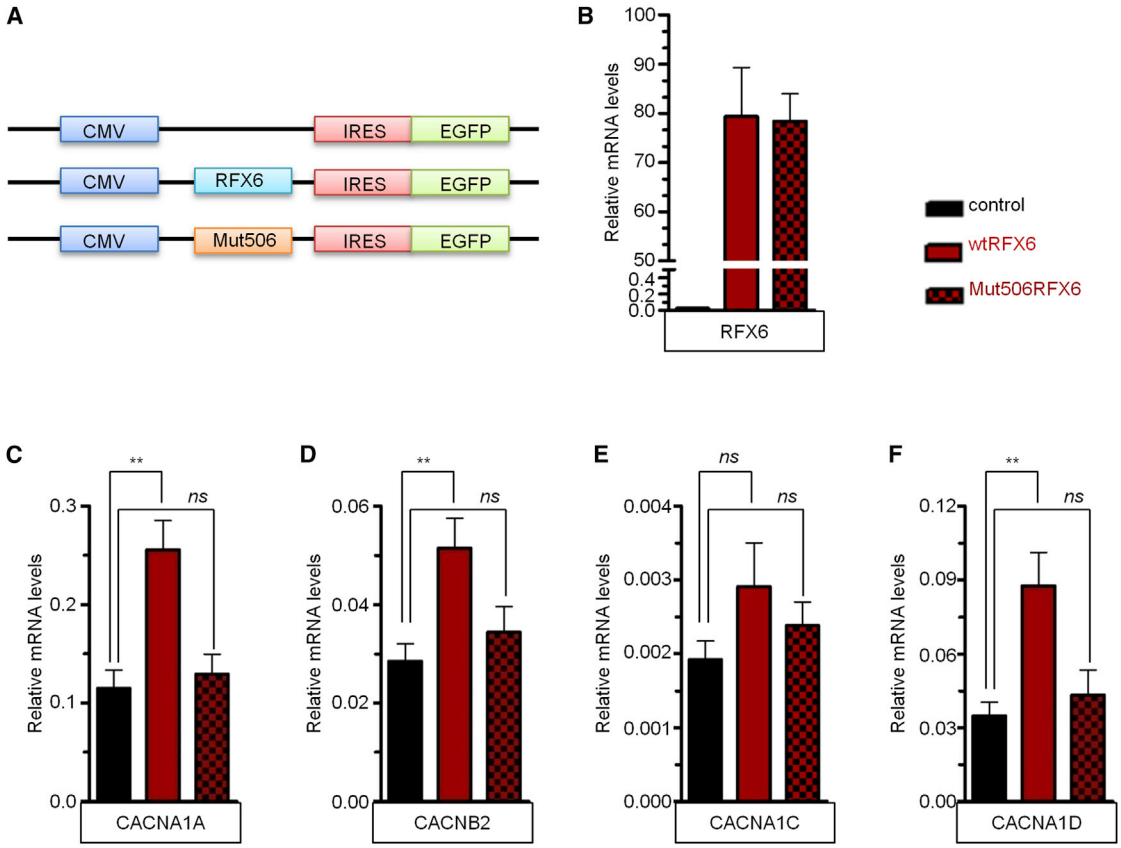

Figure 7. Differential Activation of Ca^{2+}-Channel Gene Expression by WT and Mutant RFX6 in EndoC-βH2 Cells

(A) Schematic presentation of the bicistronic constructs with IRES-EGFP used to overexpress RFX6 or Mut506 RFX6.

(B) Forty-eight hours posttransfection, GFP^+ cells were FACS isolated and analyzed by real-time qPCR for the expression of *RFX6*.

(C–F) Real-time qPCR analyses of *CACNA1A*, *CACNB2*, *CACNA1C*, and *CACNA1D* in EndoC-βH2 cells transfected with either RFX6 or Mut506 RFX6.

Data are mean ± SEM of three to five experiments. **p < 0.01; *ns*, not significant.

resulting from the 50% decrease in the *GCK* (encoding the rate-limiting glycolytic enzyme glucokinase).

Furthermore, we demonstrated that reduced RFX6 expression also decreased expression of genes encoding the voltage-gated Ca^{2+} channels. Of particular importance in this context is the reduced expression of L-type Ca^{2+}-channel genes *CACNA1C* and *CACNA1D*. This is suggested by several pieces of evidence. First, blocking L-type Ca^{2+} channels with the selective antagonist nifedipine (Figure 4A) mimicked the effect of RFX6 depletion and abolished glucose-induced insulin secretion. Second, after silencing of *RFX6*, nifedipine exerted no further inhibitory effect. Third, electrophysiological analyses of the whole-cell Ca^{2+}-current provided direct confirmation of lowered L-type (but not P/Q-type) Ca^{2+}-channel activity (Figures 5C and 5D). The reduction of L-type Ca^{2+}-channel activity is likely to account for the marked reduction of Ca^{2+}-dependent exocytosis (Figures 5E and 5F). Interestingly, we note here the presence of several X box consensus sites with high matrix similarity on 2 kb upstream sequence of P/Q-type and L-type calcium-channel genes (Figure S5), indicating the possibility of a direct regulation by RFX6, which needs to be further studied. We observed similar downregulation of these β cell-specific targets in *RFX6* knockdown human islets. This was the case for *INS*, *Pre-INS*, *CACNA1A*, *CACNB2*, *CACNA1C*, and *ABCC8*. Data presented here were obtained from a single human-islet preparation, but results are concurrent with that obtained from the β cell line. Of note, RFX6 is also expressed in human alpha cells (Figure 1A); our initial screening on *RFX6* knockdown in human islets indicates that RFX6 depletion does not modulate the expression of alpha cell-specific genes such as *Glucagon*, *ARX*, *IRX1*, and *IRX2* (data not shown). Further work is needed to define the role of RFX6 in human alpha cells. Functional human alpha cell lines, currently unavailable, would be useful for this purpose.

Thus, RFX6 regulates many key steps in the β cell stimulus-secretion coupling. This is reminiscent of what has previously been reported for other β cell transcription factors like PDX1 (Petersen et al., 1994; Waeber et al., 1996) or MAFA (Wang et al., 2007). Our data indicate that RFX6 plays a crucial role in human β cell function and it should be added to the list of major human β cell transcription factors. Surprisingly, the level of RFX6 expression is rarely measured in protocols aiming at generating functional β cells from human embryonic stem cells (hESCs) (Kroon et al., 2008; Rezania et al., 2012). Whether lack of

glucose-stimulated insulin secretion from hESCs would correlate with low levels of RFX6 needs to be tested.

It can be concluded that RFX6 regulates many steps of pancreas development (Smith et al., 2010; Soyer et al., 2010) and insulin secretion (the present study). Importantly, biallelic mutations in *RFX6* have been shown to be the cause of the Mitchell-Riley syndrome, a rare condition presenting permanent neonatal diabetes (PNDM) in human (Concepcion et al., 2014; Smith et al., 2010; Spiegel et al., 2011). PNDM is a rare monogenic form of nonautoimmune diabetes. It can be caused by either pancreas agenesis (Stoffers et al., 1997) or by an absence of β cells within the pancreas (Rubio-Cabezas et al., 2011), or by nonfunctional β cells within the pancreas (Babenko et al., 2006; Pearson et al., 2006). Here, we report the case of a young patient diagnosed with neonatal diabetes, who is a carrier of a homozygous missense mutation of *RFX6* (p.V506G). 3D MRI scanning indicated that this patient has a pancreatic gland, albeit smaller than controls (data not shown). When tested in EndoC-βH2 cells, this mutant form of RFX6 was unable to transactivate the insulin gene and to increase the mRNAs coding for β cell Ca^{2+} channels, in contrast to what was observed with control RFX6. In these assays, the RFX6-p.V506G mutant was therefore inactive. In overexpression studies, we reproducibly observed Mut506RFX6 protein level to be 39% ± 16% less compared to wtRFX6 even though the transcripts levels were comparable (Figures S7A, S7B, and 7B). These data pointed to a decreased stability of the mutant protein, as previously shown for PDX1 mutants linked to specific forms of neonatal diabetes (Schwitzgebel et al., 2003). However, cyclohexamide (CHX)-chase analysis showed comparable half-lives of ∼3–4 hr for both wtRFX6 and Mut506RFX6 proteins (Figures S7C and S7D). Moreover, a proteasome inhibitor (MG132) similarly regulated the levels of both wild-type (WT) and mutant RFX6 (Figure S7C). Thus, the mutation does not dramatically affect Mut506RFX6 protein stability. We believe that the lower expression levels of the Mut506RFX6 cannot entirely explain its almost total loss of activity in our different assays. Our data rather point on a possible qualitative alteration of the Mut506RFX6 protein. A possibility is that the p.V506G mutation affecting a highly conserved residue within the D domain of RFX6 reduces RFX6-mediated transactivation on several putative target genes as a result of impaired homo- or heterodimerization with its relatives, especially with RFX3 that has been shown to be expressed and important for pancreatic β cell function (Ait-Lounis et al., 2007, 2010).

Previous work has established that the most frequent forms of neonatal diabetes results from gain-of-function mutations in genes coding for the two subunits of the K_{ATP} channel (Ashcroft and Rorsman, 2012). In such cases, insulin is not secreted upon glucose stimulation but remains sensitive to sulfonylureas (Ashcroft, 2010). This fundamental data permitted replacement of insulin injections in such patients with sulfonylurea drugs (Babenko et al., 2006; Pearson et al., 2006). Our data obtained using a newly developed functional human β cell line (Scharfmann et al., 2014) demonstrate that mutations in *RFX6* can give rise to neonatal diabetes that is due to impaired glucose-induced insulin secretion that is secondary to reduced L-type Ca^{2+}-channel activity. It is unlikely that patients with this genetic subtype of neonatal diabetes will respond to sulphonylurea therapy. Instead, therapy should aim to restore L-type Ca^{2+}-channel activity to that seen in normal β cells. In this context, it is of interest that physiologically and therapeutically relevant concentrations of the incretin GLP-1 increase Ca^{2+}-channel activity and increase depolarization-evoked insulin exocytosis (Holz et al., 1999). This may represent a basis for treatment strategies of neonatal diabetes due to *RFX6* mutations.

EXPERIMENTAL PROCEDURES

Culture of Human Cell Lines

EndoC-βH2 cells (Scharfmann et al., 2014) were cultured in low-glucose (5.6 mM) Dulbecco's modified Eagle's medium (DMEM; Sigma-Aldrich) with 2% BSA fraction V (Roche Diagnostics), 50 μM 2-mercaptoethanol, 10 mM nicotinamide (Calbiochem), 5.5 μg/ml transferrin (Sigma-Aldrich), 6.7 ng/ml selenite (Sigma-Aldrich), 100 U/ml penicillin, and 100 μg/ml streptomycin. Cells were seeded at a density of 5×10^4 cells/cm^2 on Matrigel (1%)/fibronectin (2 μg/ml; Sigma-Aldrich) -coated plates and cultured at 37°C and 5% CO_2. The human duct cell line SKPC (Vila et al., 1994) was cultured in high-glucose DMEM supplemented with 10% fetal calf serum (Biowest) and 100 U/ml penicillin and 100 μg/ml streptomycin.

siRNA Transfection in EndoC-βH2

For siRNA-based gene knockdown, EndoC-βH2 cells were transfected using Lipofectamine RNAiMAX (Life Technologies) following manufacturer's instructions with minor modifications. Briefly, freshly trypsinized EndoC-βH2 cell suspension (5×10^4 cells/cm^2) were incubated with lipofectamine-siRNA complex in Opti-MEM containing 2-mercaptoethanol, nicotinamide, transferrin, and selenite for 3–4 min and next were plated. Three to 5 hr later, the medium was replaced. ON-TARGET*plus* siRNA SMARTpool for human RFX6 gene (∼30 nM) and ON-TARGET*plus* nontargeting pool (siNT; Dharmacon, Thermo Scientific) were used. Cells were harvested 72 hr posttransfection for further analysis. FAM-labeled siGLO Green transfection indicator (Thermo Scientific) was used to determine the transfection efficiency of EndoC-βH2 cells.

Human Genetic Analyses and *RFX6* Gene Sequencing

One female patient of West Indies origin, born from consanguineous parents and diagnosed at birth with diabetes, duodenal stenosis, and jejunal atresia, was investigated for the search of a genetic etiology. The family was referred to the French NDM study group. Informed consent for genetic analysis was obtained from the parents. Genome-wide SNP typing using Illumina Infinium660K-SNP microarrays (according to manufacturer's instructions; Illumina) was carried out in the proband and both parents in order to detect large homozygous regions (runs of homozygosity [ROHs] ≥2.5 Mb in size) that are only present in the child, as previously described for homozygosity mapping (Bonnefond et al., 2013).

Bidirectional Sanger sequencing of all exons 1–19 of the *RFX6* gene, flanking intron-exon boundaries, and the proximal promoter were performed from a PCR-amplified genomic DNA sample in the proband using the automated Applied Biosystems 3730xl DNA Analyzer (Life Technologies). Electropherogram readouts were assembled and analyzedusing the Applied Biosystems Variant Reporter software (Life Technologies).

Transcriptome Analysis and Access to Raw Data

Microarray analysis was performed according to Agilent protocol (One-Color Microarray-Based Gene Expression Analysis - Low Input Quick Amp Labeling [version 6.5, May 2010]) with Agilent SurePrint G3 Human Gene Expression 8 × 60K Microarray (Design ID 028004; see the Supplemental Experimental Procedures).

Calcium Current Measurements

Ca^{2+}-channel activity was measured using the standard whole-cell configuration of the patch-clamp technique. The extracellular medium contained (mM) 118 NaCl, 5.6 KCl, 2.6 $CaCl_2$, 1.2 $MgCl_2$, 5 HEPES (pH 7.4 using NaOH), and 3 glucose. Tetraethylammmonium (TEA)-chloride and tetrodotoxin were

included at concentrations of 20 mM and 0.1 μg/ml to block K^+ and Na^+ currents, respectively. The recording electrodes were filled with (intracellular medium; mM) 120 $CsCl_2$, 1 $MgCl_2$, 10 EGTA, 1 $CaCl_2$, 10 HEPES (pH 7.2 using CsOH), and 3 mM Mg-ATP. The Ca^{2+} channels were activated by 50 ms depolarizations from a holding potential of −70 mV to voltages between −80 mV and +40 mV (10 mV increments).

In order to identify which Ca^{2+}-channel subtypes were affected by the RFX6 downregulation, we used the specific L- and P/Q types blockers isradipine (catalog no. I-100, Alomone) and ω-agatoxin IVA (cat# RTA-500, Alomone) at concentrations of 10 μM and 200 nM, respectively, to isolate the L- and P/Q-type Ca^{2+}-current components. In these experiments, the Ca^{2+} currents were activated by voltage ramps between −80 mV and +40 mV applied at a speed of 3 V/s.

Capacitance Measurements of Exocytosis

Exocytosis was monitored in transfected EndoC-βH2 cells by measurements of membrane capacitance. The standard whole-cell configuration was used, and the pipette-filling medium contained (mM) 125 Cs-glutamate, 10 CsCl, 10 NaCl, 1 $MgCl_2$, 0.05 EGTA, 3 Mg-ATP, 0.1 cAMP, and 5 HEPES (pH 7.2 using CsOH). Ten depolarizations of 500 ms from –70 to 0 mV were applied at a frequency of 1 Hz. The responses were measured as the increase in membrane capacitance between the prestimulatory level and the new steady-state value and were normalized by the size of the cell.

Statistics

Quantitative data are presented as the mean ± SEM from at least three independent experiments, unless otherwise indicated. Statistical significances were estimated using two-tailed Student's t test. Statistical significance was set at $p < 0.05$.

ACCESSION NUMBERS

All data are MIAME compliant, and the raw data have been deposited to the NCBI Gene Expression Omnibus and are accessible under accession number GSE59049.

SUPPLEMENTAL INFORMATION

Supplemental Information includes Supplemental Experimental Procedures, seven figures, one table, and four movies and can be found with this article online at http://dx.doi.org/10.1016/j.celrep.2014.11.010.

AUTHOR CONTRIBUTIONS

V.C. designed research, performed experiments, analyzed data, and wrote the manuscript. O.A. designed experiments, analyzed data, and wrote the manuscript. B.H. performed electrophysiology experiments and contributed to the manuscript writing. J.P. analyzed transcriptome data. C.R. performed fura-2-based calcium experiments. E.V., H.C., K.B., M.V., M.P., and P.F. provided patient genetic data. P.R. analyzed electrophysiology data and wrote the manuscript. R.S. designed research, analyzed data, and wrote the manuscript.

ACKNOWLEDGMENTS

This work was supported by grants from ANR Blanc RFX-PancInt (to R.S. and M.V.), the Seventh Framework Programme of the European Union (no. 241883 to R.S.), and the Foundation Bettencourt Schueller (to R.S.). R.S.'s laboratory belongs to the Laboratoire d'Excellence consortium Revive and to the Departement Hospitalo-Universitaire (DHU) Autoimmune and Hormonal diseases. We wish to thank Dr. J.J. Robert for his help in taking care of the patient. Stéphane Lobbens and Boris Skrobek (both at the CNRS UMR 8199, Lille, France) have contributed to the ROH genetic analysis. Transcriptomic studies were performed at the Microarrays and Deep sequencing platform of the IGBMC. Electrophysiological studies in Oxford were supported by a Wellcome Trust Senior Investigator Award (to P.R.).

Received: July 31, 2014
Revised: October 9, 2014
Accepted: November 6, 2014
Published: December 11, 2014

REFERENCES

Aftab, S., Semenec, L., Chu, J.S.-C., and Chen, N. (2008). Identification and characterization of novel human tissue-specific RFX transcription factors. BMC Evol. Biol. *8*, 226.

Ahlgren, U., Jonsson, J., Jonsson, L., Simu, K., and Edlund, H. (1998). beta-cell-specific inactivation of the mouse Ipf1/Pdx1 gene results in loss of the beta-cell phenotype and maturity onset diabetes. Genes Dev. *12*, 1763–1768.

Ait-Lounis, A., Baas, D., Barras, E., Benadiba, C., Charollais, A., Nlend Nlend, R., Liègeois, D., Meda, P., Durand, B., and Reith, W. (2007). Novel function of the ciliogenic transcription factor RFX3 in development of the endocrine pancreas. Diabetes *56*, 950–959.

Ait-Lounis, A., Bonal, C., Seguín-Estévez, Q., Schmid, C.D., Bucher, P., Herrera, P.L., Durand, B., Meda, P., and Reith, W. (2010). The transcription factor Rfx3 regulates beta-cell differentiation, function, and glucokinase expression. Diabetes *59*, 1674–1685.

Arda, H.E., Benitez, C.M., and Kim, S.K. (2013). Gene regulatory networks governing pancreas development. Dev. Cell *25*, 5–13.

Ashcroft, F.M. (2010). New uses for old drugs: neonatal diabetes and sulphonylureas. Cell Metab. *11*, 179–181.

Ashcroft, F.M., and Rorsman, P. (2012). Diabetes mellitus and the β cell: the last ten years. Cell *148*, 1160–1171.

Babenko, A.P., Polak, M., Cavé, H., Busiah, K., Czernichow, P., Scharfmann, R., Bryan, J., Aguilar-Bryan, L., Vaxillaire, M., and Froguel, P. (2006). Activating mutations in the ABCC8 gene in neonatal diabetes mellitus. N. Engl. J. Med. *355*, 456–466.

Bonnefond, A., Vaillant, E., Philippe, J., Skrobek, B., Lobbens, S., Yengo, L., Huyvaert, M., Cavé, H., Busiah, K., Scharfmann, R., et al. (2013). Transcription factor gene MNX1 is a novel cause of permanent neonatal diabetes in a consanguineous family. Diabetes Metab. *39*, 276–280.

Braun, M., Ramracheya, R., Bengtsson, M., Zhang, Q., Karanauskaite, J., Partridge, C., Johnson, P.R., and Rorsman, P. (2008). Voltage-gated ion channels in human pancreatic beta-cells: electrophysiological characterization and role in insulin secretion. Diabetes *57*, 1618–1628.

Braun, M., Ramracheya, R., Johnson, P.R., and Rorsman, P. (2009). Exocytotic properties of human pancreatic beta-cells. Ann. N Y Acad. Sci. *1152*, 187–193.

Caicedo, A. (2013). Paracrine and autocrine interactions in the human islet: more than meets the eye. Semin. Cell Dev. Biol. *24*, 11–21.

Concepcion, J.P., Reh, C.S., Daniels, M., Liu, X., Paz, V.P., Ye, H., Highland, H.M., Hanis, C.L., and Greeley, S.A.W. (2014). Neonatal diabetes, gallbladder agenesis, duodenal atresia, and intestinal malrotation caused by a novel homozygous mutation in RFX6. Pediatr. Diabetes *15*, 67–72.

Dai, C., Brissova, M., Hang, Y., Thompson, C., Poffenberger, G., Shostak, A., Chen, Z., Stein, R., and Powers, A.C. (2012). Islet-enriched gene expression and glucose-induced insulin secretion in human and mouse islets. Diabetologia *55*, 707–718.

Dorrell, C., Schug, J., Lin, C.F., Canaday, P.S., Fox, A.J., Smirnova, O., Bonnah, R., Streeter, P.R., Stoeckert, C.J., Jr., Kaestner, K.H., and Grompe, M. (2011). Transcriptomes of the major human pancreatic cell types. Diabetologia *54*, 2832–2844.

Doyle, M.J., and Sussel, L. (2007). Nkx2.2 regulates β-cell function in the mature islet. Diabetes *56*, 1999–2007.

Emery, P., Durand, B., Mach, B., and Reith, W. (1996). RFX proteins, a novel family of DNA binding proteins conserved in the eukaryotic kingdom. Nucleic Acids Res. *24*, 803–807.

Evans-Molina, C., Garmey, J.C., Ketchum, R., Brayman, K.L., Deng, S., and Mirmira, R.G. (2007). Glucose regulation of insulin gene transcription and pre-mRNA processing in human islets. Diabetes *56*, 827–835.

Folias, A.E., and Hebrok, M. (2014). Diabetes. Solving human β-cell development—what does the mouse say? Nat. Rev. Endocrinol. *10*, 253–255.

Gao, T., McKenna, B., Li, C., Reichert, M., Nguyen, J., Singh, T., Yang, C., Pannikar, A., Doliba, N., Zhang, T., et al. (2014). Pdx1 maintains β cell identity and function by repressing an α cell program. Cell Metab. *19*, 259–271.

Hay, C.W., and Docherty, K. (2006). Comparative analysis of insulin gene promoters: implications for diabetes research. Diabetes *55*, 3201–3213.

Holz, G.G., Leech, C.A., Heller, R.S., Castonguay, M., and Habener, J.F. (1999). cAMP-dependent mobilization of intracellular Ca2+ stores by activation of ryanodine receptors in pancreatic beta-cells. A Ca2+ signaling system stimulated by the insulinotropic hormone glucagon-like peptide-1-(7-37). J. Biol. Chem. *274*, 14147–14156.

Kroon, E., Martinson, L.A., Kadoya, K., Bang, A.G., Kelly, O.G., Eliazer, S., Young, H., Richardson, M., Smart, N.G., Cunningham, J., et al. (2008). Pancreatic endoderm derived from human embryonic stem cells generates glucose-responsive insulin-secreting cells in vivo. Nat. Biotechnol. *26*, 443–452.

Margolin, J.F., Friedman, J.R., Meyer, W.K., Vissing, H., Thiesen, H.J., and Rauscher, F.J., 3rd. (1994). Krüppel-associated boxes are potent transcriptional repression domains. Proc. Natl. Acad. Sci. USA *91*, 4509–4513.

Pan, F.C., and Wright, C. (2011). Pancreas organogenesis: from bud to plexus to gland. Dev. Dyn. *240*, 530–565.

Papizan, J.B., Singer, R.A., Tschen, S.-I., Dhawan, S., Friel, J.M., Hipkens, S.B., Magnuson, M.A., Bhushan, A., and Sussel, L. (2011). Nkx2.2 repressor complex regulates islet β-cell specification and prevents β-to-α-cell reprogramming. Genes Dev. *25*, 2291–2305.

Pearson, E.R., Flechtner, I., Njølstad, P.R., Malecki, M.T., Flanagan, S.E., Larkin, B., Ashcroft, F.M., Klimes, I., Codner, E., Iotova, V., et al.; Neonatal Diabetes International Collaborative Group (2006). Switching from insulin to oral sulfonylureas in patients with diabetes due to Kir6.2 mutations. N. Engl. J. Med. *355*, 467–477.

Petersen, H.V., Serup, P., Leonard, J., Michelsen, B.K., and Madsen, O.D. (1994). Transcriptional regulation of the human insulin gene is dependent on the homeodomain protein STF1/IPF1 acting through the CT boxes. Proc. Natl. Acad. Sci. USA *91*, 10465–10469.

Polak, M., and Shield, J. (2004). Neonatal and very-early-onset diabetes mellitus. Semin. Neonatol. *9*, 59–65.

Reith, W., Herrero-Sanchez, C., Kobr, M., Silacci, P., Berte, C., Barras, E., Fey, S., and Mach, B. (1990). MHC class II regulatory factor RFX has a novel DNA-binding domain and a functionally independent dimerization domain. Genes Dev. *4*, 1528–1540.

Rezania, A., Bruin, J.E., Riedel, M.J., Mojibian, M., Asadi, A., Xu, J., Gauvin, R., Narayan, K., Karanu, F., O'Neil, J.J., et al. (2012). Maturation of human embryonic stem cell-derived pancreatic progenitors into functional islets capable of treating pre-existing diabetes in mice. Diabetes *61*, 2016–2029.

Rorsman, P. (1997). The pancreatic beta-cell as a fuel sensor: an electrophysiologist's viewpoint. Diabetologia *40*, 487–495.

Rorsman, P., and Braun, M. (2013). Regulation of insulin secretion in human pancreatic islets. Annu. Rev. Physiol. *75*, 155–179.

Rubio-Cabezas, O., Jensen, J.N., Hodgson, M.I., Codner, E., Ellard, S., Serup, P., and Hattersley, A.T. (2011). Permanent Neonatal Diabetes and Enteric Anendocrinosis Associated With Biallelic Mutations in NEUROG3. Diabetes *60*, 1349–1353.

Scharfmann, R., Rachdi, L., and Ravassard, P. (2013). Concise review: in search of unlimited sources of functional human pancreatic beta cells. Stem Cells Transl Med *2*, 61–67.

Scharfmann, R., Pechberty, S., Hazhouz, Y., von Bülow, M., Bricout-Neveu, E., Grenier-Godard, M., Guez, F., Rachdi, L., Lohmann, M., Czernichow, P., and Ravassard, P. (2014). Development of a conditionally immortalized human pancreatic β cell line. J. Clin. Invest. *124*, 2087–2098.

Schulla, V., Renström, E., Feil, R., Feil, S., Franklin, I., Gjinovci, A., Jing, X.-J., Laux, D., Lundquist, I., Magnuson, M.A., et al. (2003). Impaired insulin secretion and glucose tolerance in beta cell-selective Ca(v)1.2 Ca2+ channel null mice. EMBO J. *22*, 3844–3854.

Schwitzgebel, V.M., Mamin, A., Brun, T., Ritz-Laser, B., Zaiko, M., Maret, A., Jornayvaz, F.R., Theintz, G.E., Michielin, O., Melloul, D., and Philippe, J. (2003). Agenesis of human pancreas due to decreased half-life of insulin promoter factor 1. J. Clin. Endocrinol. Metab. *88*, 4398–4406.

Smith, S.B., Qu, H.-Q., Taleb, N., Kishimoto, N.Y., Scheel, D.W., Lu, Y., Patch, A.-M., Grabs, R., Wang, J., Lynn, F.C., et al. (2010). Rfx6 directs islet formation and insulin production in mice and humans. Nature *463*, 775–780.

Soyer, J., Flasse, L., Raffelsberger, W., Beucher, A., Orvain, C., Peers, B., Ravassard, P., Vermot, J., Voz, M.L., Mellitzer, G., and Gradwohl, G. (2010). Rfx6 is an Ngn3-dependent winged helix transcription factor required for pancreatic islet cell development. Development *137*, 203–212.

Spiegel, R., Dobbie, A., Hartman, C., de Vries, L., Ellard, S., and Shalev, S.A. (2011). Clinical characterization of a newly described neonatal diabetes syndrome caused by RFX6 mutations. Am. J. Med. Genet. A. *155A*, 2821–2825.

Stoffers, D.A., Zinkin, N.T., Stanojevic, V., Clarke, W.L., and Habener, J.F. (1997). Pancreatic agenesis attributable to a single nucleotide deletion in the human IPF1 gene coding sequence. Nat. Genet. *15*, 106–110.

Taylor, B.L., Liu, F.-F., and Sander, M. (2013). Nkx6.1 is essential for maintaining the functional state of pancreatic beta cells. Cell Rep *4*, 1262–1275.

Vaxillaire, M., Bonnefond, A., and Froguel, P. (2012). The lessons of early-onset monogenic diabetes for the understanding of diabetes pathogenesis. Best Pract. Res. Clin. Endocrinol. Metab. *26*, 171–187.

Vila, M.R., Lloreta, J., and Real, F.X. (1994). Normal human pancreas cultures display functional ductal characteristics. Lab. Invest. *71*, 423–431.

Waeber, G., Thompson, N., Nicod, P., and Bonny, C. (1996). Transcriptional activation of the GLUT2 gene by the IPF-1/STF-1/IDX-1 homeobox factor. Mol. Endocrinol. *10*, 1327–1334.

Wang, H., Brun, T., Kataoka, K., Sharma, A.J., and Wollheim, C.B. (2007). MAFA controls genes implicated in insulin biosynthesis and secretion. Diabetologia *50*, 348–358.